Electronic Supplementary Material (ESI) for Physical Chemistry Chemical Physics.

Electronic Supplementary Information for: Role of metcar on the adsorption and activation of carbon dioxide: A DFT Study

Megha,[a‡] Arup Banerjee,[a‡] and Tapan K. Ghanty*[bc‡]

[a] *Human Resources Development Section, Raja Ramanna Centre for Advanced Technology, Indore 452013, India.*
[b] *Theoretical Chemistry Section, Chemistry Group, Bhabha Atomic Research Centre, Mumbai 400085, India.*
[c] *Bio-Science Group, Bhabha Atomic Research Centre, Mumbai 400085, India. Email: tapang@barc.gov.in*
[‡] *Homi Bhabha National Institute, Training School Complex, Anushaktinagar, Mumbai 400094, India.*

Contents

List of Figures

List of Tables

1 Geometric and electronic characterization of bare Ti_8C_{12} cluster

In the Tables S4 and S5, we present the results obtained with LDZ and Def2 basis sets and the XC functionals PBE, PBE0, B3LYP, and TPSS for various geometric and electronic properties of the lowest energy isomer with C_{3v} symmetry. As, we can see from Tables S4 and S5 that the spin contamination for the most stable isomer of Ti_8C_{12} cluster is more pronounced with hybrid XC functionals (B3LY and PBE0) than that with GGA (PBE) and meta-GGA (TPSS) functionals, which is also in accordance with the already reported results by Schmidt and co-workers[7].

We note from Table S6 that for both the isomers of Ti_8C_{12} metcar, the Ti^o-Ti^o bond distance is almost two times the distance between two Ti^i atoms because the inner Ti atoms are directly connected to each other whereas outer Ti atoms are connected through a C_2 unit (see Fig. 1). We further observe from Table S6 that for the isomer with C_{3v} symmetry, the bond distances between all the Ti^o atoms are nearly equal, indicating that the outer tetrahedron becomes a sub-unit which is close to a structure with T_d symmetry. However, the distance between inner Ti atoms varies between 2.81 and 2.98 Å (with B3LYP) and 2.72 and 2.90 Å (with PBE), indicating that the inner tetrahedron gets distorted in case of isomer with C_{3v} symmetry. Unlike the isomer with C_{3v} symmetry we observe that the distances between all Ti^o atoms of the isomer with D_{2d} symmetry are equal, indicating a perfect outer tetrahedron. Whereas like C_{3v} isomer, the inner tetrahedron gets distorted for D_{2d} isomer also. It can be further seen from Table S6 that for both the isomers, the bond distance between outer Ti atom and a C atom is small relative to that between an inner Ti atom and a C atom. It indicates that outer Ti atoms strongly interact with C atoms compared to the inner Ti atoms.

The IR spectra of a cluster provides valuable information about its geometry and can also be used to identify the corresponding structure experimentally[8]. To this end, we present the IR spectra of the two isomers (with C_{3v} and D_{2d} symmetries) of Ti_8C_{12} cluster obtained at B3LYP level along with the corresponding experimental spectra (taken from Ref. 1) in Fig. S2. Likewise, the IR spectra of the isomer with C_{3v} symmetry obtained using PBE XC functional is displayed in Fig. S3. As, the data for experimental spectra is available within 400 - 1600 cm^{-1} frequency range, so the experimental plot shown in Fig. S2 is absent beyond this frequency range. Here we wish to mention that in Fig. S2 the plots shown by magenta and blue color solid lines are broadened with Gaussian of FWHM of 8 and 40 cm^{-1}, respectively.

It has been observed in the literature that fundamental vibrational frequencies obtained using *ab initio* method are generally larger than the corresponding experimentally observed modes[9] particularly due to the use of approximate electron correlation and the incorporation of finite basis sets. But this overestimation of the

vibrational modes, in general, does not vary from system to system, therefore we can scale the theoretical frequencies calculated using *ab initio* method in order to make good match between scaled theoretically computed data and the corresponding experimental frequencies. Keeping this in mind, we scale our theoretically computed frequencies with B3LYP XC functional by a factor of 0.9297 so as to obtain a good agreement between our data and the experimental peak at 1395 cm^{-1} corresponding to C-C stretching[10]. The frequency scaling factor which we used in our work lies between the corresponding scaling factors recommended for the HF/6-31G(d) (0.8929) and MP2/6-31G(d) (0.9427) levels of theories[11]. This scaling of frequencies does not affect the overall shapes of the IR spectra, and we can see from the blue plots shown in Fig. S2 that our spectra match very well with the experimental one in the higher frequency region. Further, the experimental spectrum shows the presence of a shoulder peak near 1340 cm^{-1}, which is absent for D_{2d} isomer but such peak can be seen very clearly at 1357 cm^{-1} in the IR spectra of C_{3v} structure displayed in Fig. S2. Moreover, in the low frequency region there is a small peak at 521 cm^{-1} in the experimental spectrum which corresponds to the stretching of Ti-C bond. Similar small peaks are also observed in our computed frequency spectra (scaled) at 577 and 571 cm^{-1} for C_{3v} and D_{2d} isomers, respectively. We further observe a small peak nearly at 440 cm^{-1}, corresponding to Ti-Ti bond stretching, for both the isomers of Ti_8C_{12} cluster, which is non-degenerate in case of C_{3v} structure and doubly degenerate for D_{2d} isomer. It can also be noted that in our calculated spectra there are more peaks in the frequency region below 400 cm^{-1} which are absent in the corresponding experimental plot. However, these small peaks may appear in the experimental spectra also if the experiment is performed for the frequencies below 400 cm^{-1}. From the above results we infer that overall the IR spectra of both the isomers of Ti_8C_{12} metcar match quite well with the experimental results. However, the presence of a shoulder peak in the high frequency region is only reproduced for the isomer with C_{3v} symmetry. Therefore, we conclude that the isomer with C_{3v} symmetry is most probably the lowest energy isomer for Ti_8C_{12} metcar.

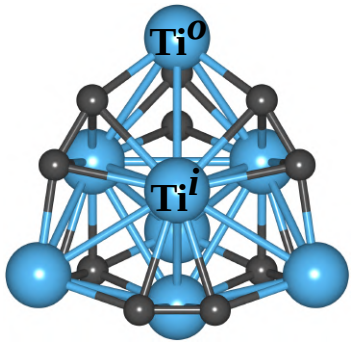

C_{3v} (0.00)

Fig. S1 Optimized structures of pristine Ti_8C_{12} metcar using LDZ and PBE XC functional. Ti^o and Ti^i correspond to the Ti atoms of the outer and inner tetrahedrons, respectively. The symmetry of the isomer is written at the bottom. The value of spin multiplicity (2S+1) of this isomer is 3. Blue and grey balls represent Ti and C atoms, respectively.

2 IR spectra of the CO_2 molecule chemisorbed onto Ti_8C_{12} metcar

In Fig. S6 we display the IR spectra for isolated CO_2 molecule along with the corresponding spectra for chemisorbed CO_2 on both the isomers (*A* and *B*) of Ti_8C_{12}-CO_2 complex. We find that a free CO_2 molecule possess two distinct vibrational modes corresponding to asymmetric and symmetric stretching of C-O bonds (centred at 2421 cm^{-1} and 1378 cm^{-1}, respectively), and two bending modes which are centred at 675 cm^{-1}, calculated with B3LYP XC functional. Since symmetric stretching of the C-O bonds of linear CO_2 molecule does not change the dipole moment so this mode is IR inactive for free CO_2 and hence this band is absent from the IR spectra of the isolated CO_2 (see Fig. S6). We observe from the IR spectra of CO_2 molecule adsorbed on isomer *A* of Ti_8C_{12}-CO_2 complex that there is a blue-shift in the signal corresponding to the bending of CO_2, that is, bending mode is now centred at 765 cm^{-1}. On the other hand, a red-shift is observed in the asymmetric stretching of C-O bonds, meaning this mode is shifted to the lower frequency value (1748 cm^{-1}) in comparison to the linear CO_2 molecule (2421 cm^{-1}). Further, for *A* isomer an additional signal, centred at 1087 cm^{-1}, can be seen from Fig. S6. This additional signal for chemisorbed CO_2 represents a symmetrical stretching of C-O bond and its occurrence in Ti_8C_{12}-CO_2 cluster-molecule complex is also consistent with the earlier theoretical and experimental IR spectra of CO_2 chemisorbed onto four-atom monometallic and bimetallic clusters[12,13]. This additional peak is red shifted in comparison to the corresponding peak which occurs at 1378 cm^{-1} for a free CO_2 molecule. It can be seen from IR spectra of isomer *A* that there are additional signals in between asymmetric and symmetric stretching modes of CO_2 which correspond to C-C stretching of the C atoms which are present in the titanium metcar. The new signals appearing between

symmetric stretching and bending modes represent the mixed vibrations within CO_2 molecule and that of C-C bond between the C atom of CO_2 and C atom of the titanium cluster. The series of small peaks in lower frequency region lying on the left side of bending mode of CO_2 indicate the stretching of Ti-C bonds (Ti: Ti^o/Ti^i) of metcar.

For isomer *B*, we find a blue shift in the signal corresponding to the mode representing the bending of chemisorbed CO_2 molecule. This signal is centred at 729 cm^{-1} and at this frequency small vibrations indicating the stretching of Ti^i-C bonds of Ti_8C_{12}-CO_2 complex are also present. We note that the asymmetric stretching mode for CO_2 molecule adsorbed on isomer *B* appears at a much lower frequency (1366 cm^{-1}) in comparison to the corresponding mode in isomer *A* (1748 cm^{-1}). Further, for isomer *B* we observe an additional signal centred at 922 cm^{-1}. This signal corresponds to the mixed vibrations of the symmetric stretching of C-O bond of chemisorbed CO_2 and the C-C bond between C atom of adsorbed CO_2 and C atom of Ti_8C_{12} cluster. Since the CO_2 molecule adsorbed on isomer *B* is coordinated with more number of atoms of Ti_8C_{12} cluster than that on isomer *A*, this may be the reason behind the additional C-C and Ti^i-C bonds vibrations appearing at symmetric stretching and bending modes in case of isomer *B*. It can further be seen from the IR spectra of isomer *B* that peaks on the right side of asymmetric stretching mode belongs to the stretching of C_2 units of metcar. However, a strong signal at 1174 cm^{-1} corresponds to the mixed vibrations of the asymmetric stretching of adsorbed CO_2 molecule and the C-C bond between the C atom of CO_2 and C atom of metcar with which CO_2 is coordinated. From these results for IR spectra of chemisorbed and linear CO_2 molecule, we infer that the red shifted additional signal, indicating the symmetric stretching of C-O bonds, occurred approximately at 1000 cm^{-1} for isomers *A* and *B* can be used as a signature for characterizing the activation of CO_2 adsorbed onto Ti_8C_{12} metcar.

Table S1 Symmetry, spin multiplicity (SM), relative energy (E_{rel}), and vibrational frequency of various isomers of pristine Ti_8C_{12} metcar optimized with LDZ basis set.

symmetry (initial structure)	method	SM (2S+1)	symmetry (optimized structure)	E_{rel} (eV)	frequency[a] (cm^{-1})
C_{3v}	PBE	3	C_{3v}	0.00	all +ve
	PBE0	3	C_{3v}	0.00	all +ve
	B3LYP	3	C_{3v}	0.00	all +ve
	TPSS	3	C_{3v}	0.00	all +ve
C_{2v}	PBE	3	C_{2v}	0.11	-177, -172
	PBE0	3	C_s	0.07	-767
	B3LYP	1	C_{2v}	0.53	all +ve
	TPSS	1	C_s	0.25	-55
D_{2d}	PBE	5	C_s	1.33	all +ve
	PBE0	3	D_{2d}	0.32	all +ve
	B3LYP	3	D_{2d}	0.29	all +ve
	TPss	3	C_s	0.03	-141
D_2	PBE	5	C_1	1.33	all +ve
	PBE0	3	C_1	0.32	all +ve
	B3LYP	3	C_1	0.29	all +ve
	TPSS	3	C_1	0.17	all +ve
D_{2h}	PBE	5	C_1	2.81	all +ve
	PBE0	1	C_1	4.24	all +ve
	B3LYP	1	C_I	3.06	all +ve
	TPSS	1	C_I	2.85	all +ve
T_d	PBE	3	C_1	0.11	-489, -488
	PBE0	3	C_1	0.32	all +ve
	B3LYP	3	D_{2d}	0.29	all +ve
	TPSS	3	C_1	0.00	all +ve
T_h	PBE	5	C_I	2.84	all +ve
	PBE0	3	C_I	3.20	-136
	B3LYP	1	C_I	3.20	-169
	TPSS	3	C_I	2.74	all +ve

[a] "all +ve" means all the corresponding vibrational frequency modes are real. Negative numbers represent the imaginary frequency modes of the corresponding structure.

Table S2 Symmetry, spin multiplicity (SM), relative energy (E_{rel}), and vibrational frequency of various isomers of pristine Ti_8C_{12} metcar optimized with LTZ basis set and B3LYP XC functional. [Values in parentheses are obtained with PBE functional]

symmetry (initial structure)	SM (2S+1)	symmetry (optimized structure)	E_{rel} (eV)	frequency (cm^{-1})
C_{3v}	3 (3)	C_{3v} (C_{3v})	0.00 (0.00)	all +ve (all +ve)
C_{2v}	3 (3)	C_{2v} (C_{2v})	0.29 (0.01)	all +ve (all +ve)
D_{2d}	3 (3)	C_1 (C_s)	0.29 (0.00)	all +ve (all +ve)
D_2	3 (3)	C_1 (C_1)	0.29 (0.01)	all +ve (all +ve)
D_{2h}	1 (5)	C_I (C_I)	3.67 (2.52)	all +ve (all +ve)
T_d	1 (5)	C_1 (C_1)	0.54 (1.29)	all +ve (all +ve)
T_h	1 (3)	C_I (C_I)	2.91 (2.24)	-156 (all +ve)

[a] "all +ve" means all the corresponding vibrational frequency modes are real. Negative numbers represent the imaginary frequency modes of the corresponding structure.

Table S3 Symmetry, spin multiplicity (SM), relative energy (E_{rel}), and vibrational frequency of various isomers of pristine Ti_8C_{12} metcar optimized with Def2 basis set.

symmetry (initial structure)	method	SM (2S+1)	symmetry (optimized structure)	E_{rel} (eV)	frequency[a] (cm^{-1})
C_{3v}	PBE	3	C_{3v}	0.00	all +ve
	PBE0	3	C_{3v}	0.00	all +ve
	B3LYP	3	C_{3v}	0.00	all +ve
	TPSS	3	C_{3v}	0.00	all +ve
C_{2v}	PBE	3	C_s	0.03	-163, -152
	PBE0	1	C_s	0.56	all +ve
	B3LYP	1	C_s	0.50	all +ve
	TPSS	3	C_s	0.11	-205, -127
D_{2d}	PBE	3	C_s	0.01	-109
	PBE0	3	C_s	0.00	all +ve
	B3LYP	3	C_s	0.00	all +ve
	TPSS	3	C_s	0.02	-135
D_2	PBE	3	C_1	0.00	all +ve
	PBE0	3	C_1	0.00	all +ve
	B3LYP	3	C_1	0.27	all +ve
	TPSS	3	C_1	0.11	-203, -121
D_{2h}	PBE	3	C_I	2.31	all +ve
	PBE0	3	C_1	1.39	all +ve
	B3LYP	3	C_1	1.45	all +ve
	TPSS	3	C_I	2.34	all +ve
T_d	PBE	3	C_1	0.00	all +ve
	PBE0	3	C_1	0.00	all +ve
	B3LYP	3	C_1	0.27	all +ve
	TPSS	3	C_s	0.11	-205, -127
T_h	PBE	3	C_I	2.10	all +ve
	PBE0	1	C_I	3.94	all +ve
	B3LYP	1	C_1	1.78	all +ve
	TPSS	3	C_I	2.40	-787

[a] "all +ve" means all the corresponding vibrational frequency modes are real. Negative numbers represent the imaginary frequency modes of the corresponding structure.

Table S4 Calculated and experimental values of the geometrical and electronic characteristics of the lowest energy isomer (with C_{3v} symmetry) of Ti_8C_{12} metcar. [$<\mathbf{S}^2>$ = S(S+1); S = spin]

	LDZ (Ti: LANL2DZ; C, O: TZVP)				
property[a]	PBE	PBE0	B3LYP	TPSS	reported
SM (2S+1)	3	3	3	3	1[2]
$<\mathbf{S}^2>$	2.0213	2.1779	2.1736	2.0340	
State	$^3A_1$	$^3A_1$	$^3A_1$	$^3A_1$	
Ti^o-Ti^o (Å)	4.87-4.90	4.83-4.84	4.85-4.86	4.86-4.89	4.92-4.94[2]
Ti^i-Ti^i (Å)	2.72-2.90	2.77-2.94	2.81-2.98	2.70-2.90	2.77-2.96[2]
Ti^o-Ti^i (Å)	2.88-2.93	2.90-2.91	2.88-2.93	2.90-2.93	2.92-2.97[2]
Ti^o-C (Å)	1.95-1.96	1.94	1.96	1.96-1.97	1.99-2.00[2]
Ti^i-C (Å)	2.20-2.22	2.20-2.21	2.21-2.23	2.21-2.23	2.24-2.27[2]
C-C (Å)	1.34	1.33	1.32-1.33	1.34	1.34-1.35[2]
BE (eV)	6.35	5.85	5.62	6.13	6.36[2]
E_{hl} (eV)	0.22	1.88	1.60	0.39	0.12[3]
VIP (eV)	4.77	5.24	4.91	4.73	4.61[3],[4.9±0.2[4]]
VEA (eV)	0.99	0.82	0.51	0.83	0.89[3], [1.16±0.05[5]]

[a] Ti^o and Ti^i correspond to Ti atoms of the outer and inner tetrahedrons, respectively. All the reported numbers are taken from the theoretical calculations except for the numerical values given within the square bracket which correspond to the experimental data. The ideal value of $<\mathbf{S}^2>$ is 2. "State" denotes the electronic state of the cluster.

Ref. 2: Method - RPBE, Basis - Double numerical plus d-functions
Ref. 3: Method - DFT, Basis - Gaussian basis set centered at atoms
Ref. 4: Method - Near-threshold Photoionization
Ref. 5: Method - Photoelectron spectroscopy
Ref. 6: Method - Spin-polarized DFT, Basis - DZVP

Table S5 Calculated and experimental values of the geometrical and electronic characteristics of the lowest energy isomer (with C_{3v} symmetry) of Ti_8C_{12} metcar. [$<\mathbf{S}^2>$ = S(S+1); S = spin]

	Def2 (Ti: Def2TZVP; C, O: TZVP)				
property[a]	PBE	PBE0	B3LYP	TPSS	reported
SM (2S+1)	3	3	3	3	1[2]
$<\mathbf{S}^2>$	2.0186	2.1775	2.1582	2.0268	
State	$^3A_1$	$^3A_1$	$^3A_1$	$^3A_1$	
Ti^o-Ti^o (Å)	4.88-4.91	4.84-4.85	4.86-4.88	4.88-4.90	4.92-4.94[2]
Ti^i-Ti^i (Å)	2.73-2.91	2.79-2.95	2.83-2.99	2.71-2.90	2.77-2.96[2]
Ti^o-Ti^i (Å)	2.91-2.94	2.91-2.92	2.93-2.94	2.91-2.94	2.92-2.97[2]
Ti^o-C (Å)	1.96-1.97	1.95	1.97	1.97-1.98	1.99-2.00[2]
Ti^i-C (Å)	2.22-2.23	2.21-2.22	2.23-2.24	2.22-2.24	2.24-2.27[2]
C-C (Å)	1.34	1.33	1.33	1.34	1.34-1.35[2]
BE (eV)	6.40	5.89	5.66	6.19	6.36[2]
E_{hl} (eV)	0.12	1.80	1.49	0.28	0.12[3]
VIP (eV)	4.57	4.55	4.62	4.51	4.61[3],[4.9±0.2[4]]
VEA (eV)	0.92	0.73	0.80	0.74	0.89[3], [1.16±0.05[5]]

[a] Ti^o and Ti^i correspond to Ti atoms of the outer and inner tetrahedrons, respectively. All the reported numbers are taken from the theoretical calculations except for the numerical values given within the square bracket which correspond to the experimental data. The ideal value of $<\mathbf{S}^2>$ is 2. "State" denotes the electronic state of the cluster.

Ref. 2: Method - RPBE, Basis - Double numerical plus d-functions
Ref. 3: Method - DFT, Basis - Gaussian basis set centered at atoms
Ref. 4: Method - Near-threshold Photoionization
Ref. 5: Method - Photoelectron spectroscopy
Ref. 6: Method - Spin-polarized DFT, Basis - DZVP

Table S6 Calculated and experimental values of the geometrical and electronic characteristics of two lowest energy isomers of Ti_8C_{12} metcar (with LDZ basis set)

symmetry	property[a]	B3LYP	PBE	PBE0	reported
C_{3v}	SM (2S+1)	3	3	3	1[2]
	Ti^o-Ti^o (Å)	4.85-4.86	4.87-4.90	4.83-4.84	4.92-4.94[2]
	Ti^i-Ti^i (Å)	2.81-2.98	2.72-2.90	2.77-2.94	2.77-2.96[2]
	Ti^o-Ti^i (Å)	2.88-2.93	2.88-2.93	2.90-2.91	2.92-2.97[2]
	Ti^o-C (Å)	1.96	1.95-1.96	1.94	1.99-2.00[2]
	Ti^i-C (Å)	2.21-2.23	2.20-2.22	2.20-2.21	2.24-2.27[2]
	C-C (Å)	1.32-1.33	1.34	1.33	1.34-1.35[2]
	BE (eV)	5.62	6.35	5.85	6.36[2]
	E_{hl} (eV)	1.60	0.22	1.88	0.12[3]
	VIP (eV)	4.91	4.77	5.24	4.61[3], [4.9±0.2[4]]
	VEA (eV)	0.51	0.99	0.82	0.89[3], [1.16±0.05[5]]
D_{2d}	SM (2S+1)	3		3	1[6]
	Ti^o-Ti^o (Å)	4.86		4.83-4.84	
	Ti^i-Ti^i (Å)	2.86-2.90		2.82-2.86	
	Ti^o-Ti^i (Å)	2.88-2.92		2.87-2.90	2.77-2.81[6]
	Ti^o-C (Å)	1.95-1.96		1.93-1.94	1.95-2.09[6]
	Ti^i-C (Å)	2.21-2.22		2.19-2.20	2.04-2.08[6]
	C-C (Å)	1.32-1.33		1.33	1.36-1.37[6]
	BE (eV)	5.60		5.84	6.54[6]
	E_{hl} (eV)	1.33		1.59	0.13[3]
	VIP (eV)	4.53		4.41	4.51[3], [4.9±0.2[4]]
	VEA (eV)	0.97		0.71	0.93[3], [1.16±0.05[5]]

[a] Ti^o and Ti^i correspond to Ti atoms of the outer and inner tetrahedrons, respectively. All the reported numbers are taken from the theoretical calculations except for the numerical values given within the square bracket which correspond to the experimental data.

Ref. 2: Method - RPBE, Basis - Double numerical plus d-functions

Ref. 3: Method - DFT, Basis - Gaussian basis set centered at atoms

Ref. 4: Method - Near-threshold Photoionization

Ref. 5: Method - Photoelectron spectroscopy

Ref. 6: Method - Spin-polarized DFT, Basis - DZVP

Table S7 Coordinates of the lowest energy isomer of Ti_8C_{12} metcar with $C3v$ point group symmetry obtained with PBE0 XC functional and LDZ basis set.

Ti_8C_{12} (C_{3v})			
C	2.145450	-0.469543	-1.486802
C	1.479361	-1.623243	-1.486802
C	0.000000	-1.701268	1.993911
C	0.000000	-2.477238	0.916361
C	-1.479361	-1.623243	-1.486802
C	-2.145450	-0.469543	-1.486802
C	0.666089	2.092786	-1.486802
C	-0.666089	2.092786	-1.486802
C	-2.145351	1.238619	0.916361
C	-1.473341	0.850634	1.993911
C	2.145351	1.238619	0.916361
C	1.473341	0.850634	1.993911
Ti	0.000000	1.703349	0.584320
Ti	-2.424077	1.399542	-1.005121
Ti	2.424077	1.399542	-1.005121
Ti	0.000000	0.000000	2.941214
Ti	1.475143	-0.851674	0.584320
Ti	0.000000	0.000000	-1.626993
Ti	-1.475143	-0.851674	0.584320
Ti	-0.000000	-2.799083	-1.005121

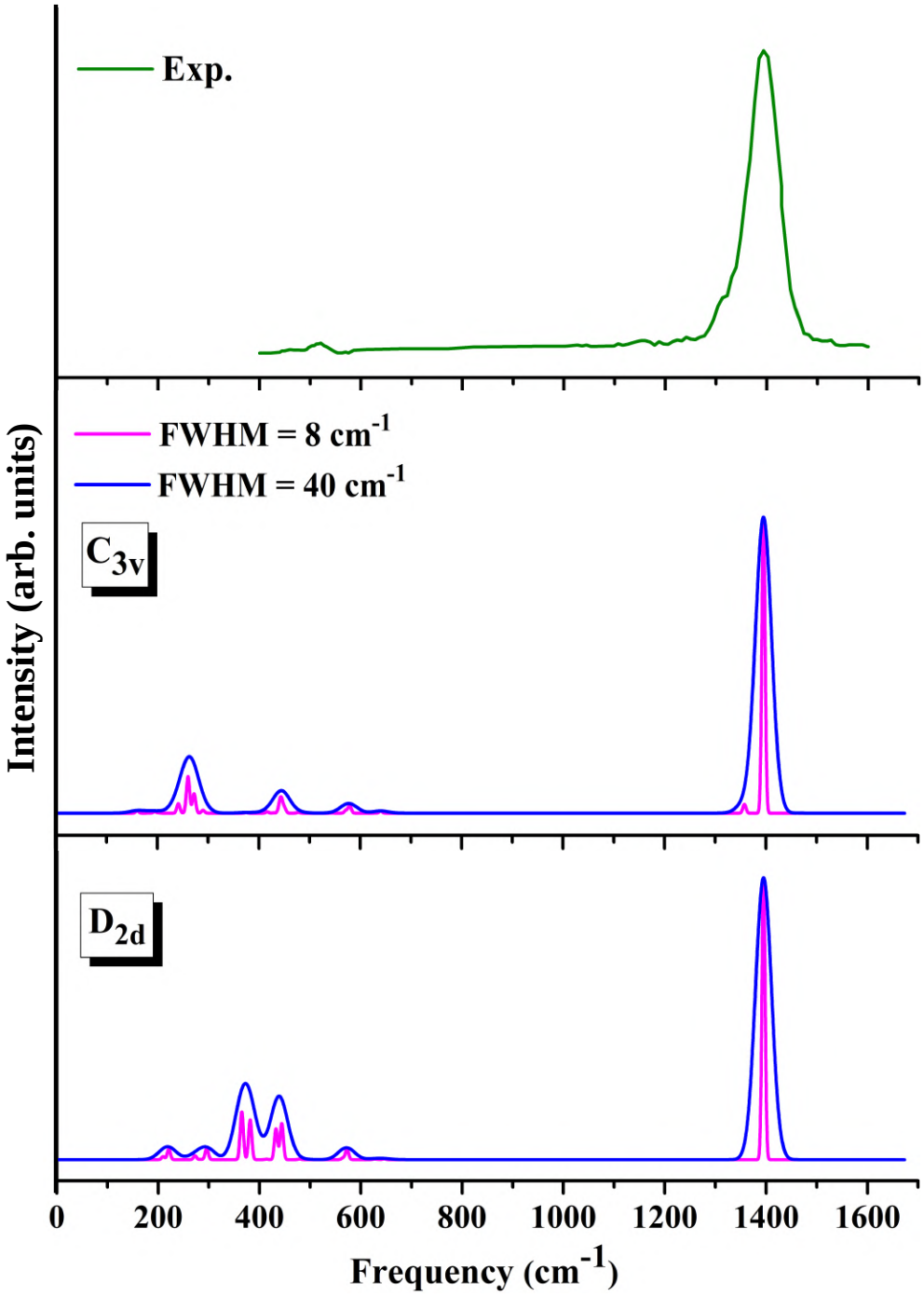

Fig. S2 Infrared spectra of two lowest energy isomers of Ti_8C_{12} met-car obtained using B3LYP XC functional and LDZ basis set together with the experimental data taken from Ref. 1.

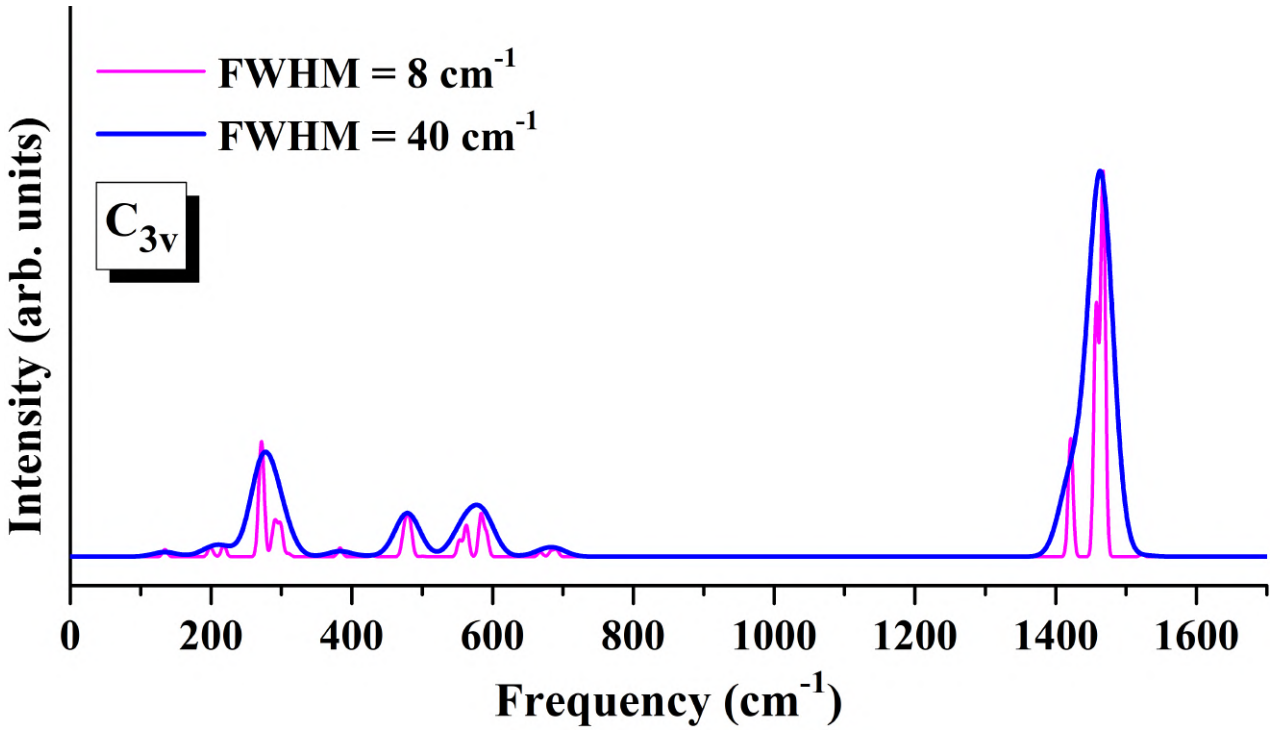

Fig. S3 Infrared spectra of the lowest energy isomer of Ti_8C_{12} met-car obtained using PBE XC functional and LDZ basis set.

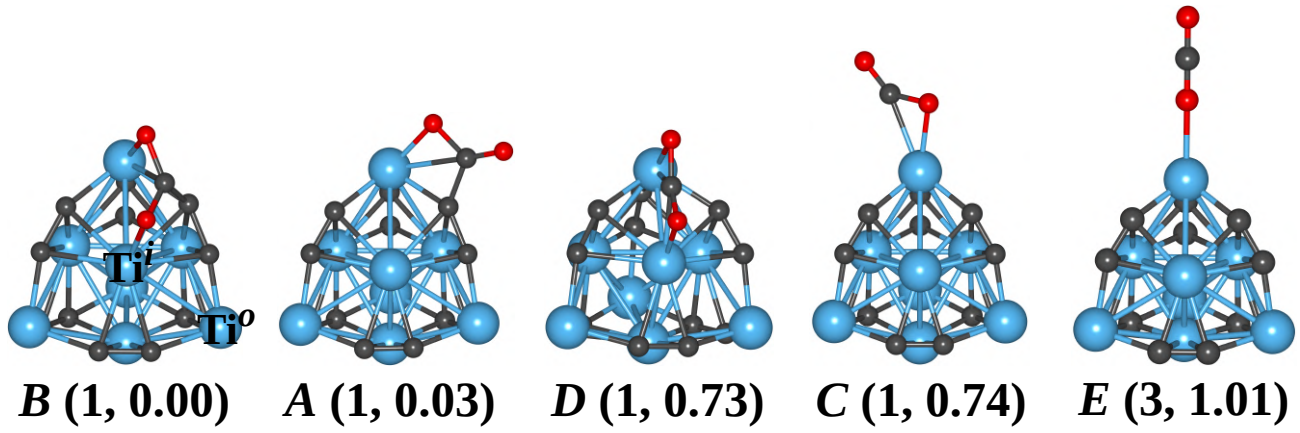

Fig. S4 Optimized structures of Ti_8C_{12}-CO_2 cluster-molecule complex using PBE XC functional and LDZ basis set. The first number within the parentheses corresponds to the spin multiplicity (2S+1) and the second number denotes the relative energy (in eV) of the Ti_8C_{12}-CO_2 complexes with respect to the most stable isomer *B*. Ti^o and Ti^i correspond to the Ti atoms of the outer and inner tetrahedrons, respectively. Blue, grey, and red balls represent Ti, C, and O atoms, respectively.

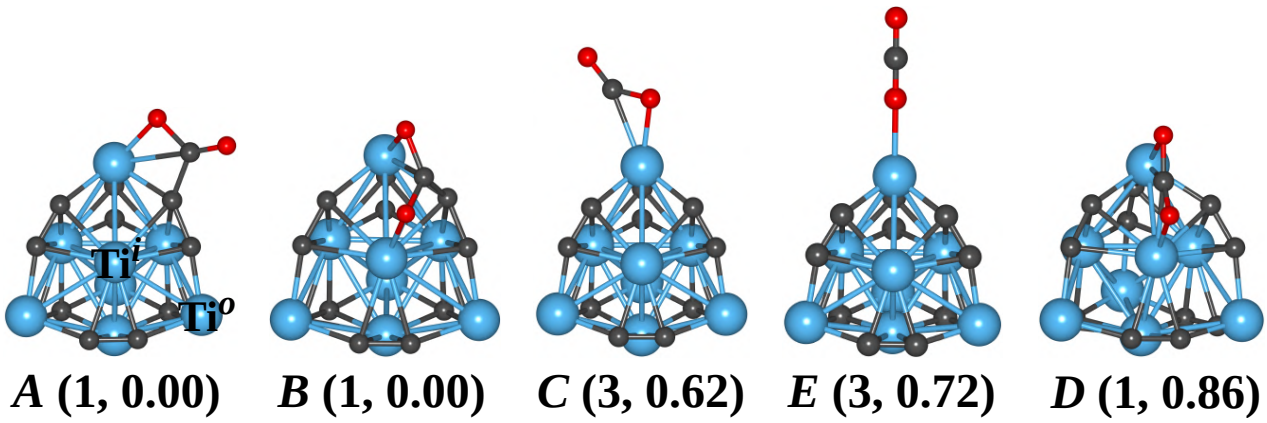

Fig. S5 Optimized structures of Ti_8C_{12}-CO_2 cluster-molecule complex using PBE0 XC functional and LDZ basis set. The first number within the parentheses corresponds to the spin multiplicity (2S+1) and the second number denotes the relative energy (in eV) of the Ti_8C_{12}-CO_2 complexes with respect to the most stable isomer *A*. Ti^o and Ti^i correspond to the Ti atoms of the outer and inner tetrahedrons, respectively. Blue, grey, and red balls represent Ti, C, and O atoms, respectively.

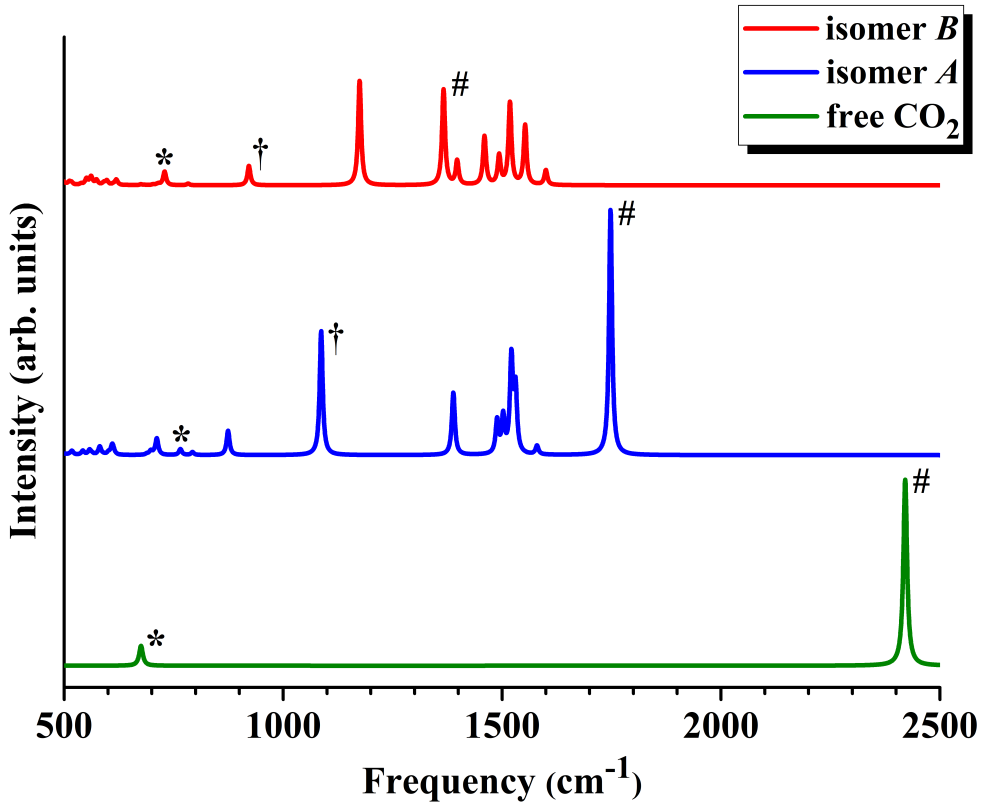

Fig. S6 Infrared spectra for the lowest energy structures of Ti_8C_{12}-CO_2 complex together with the corresponding spectra for gas phase CO_2 obtained with B3LYP functional and LDZ basis set. The symbols (*), (†), and (#) separately denotes the bending, symmetric stretching, and asymmetric stretching modes of CO_2 molecule.

Table S8 Coordinates of the various isomers of Ti_8C_{12}-CO_2 complex optimized with PBE0 XC functional and LDZ basis set.

Ti_8C_{12}-CO_2 (*A*)			
C	-1.456581	-1.628280	-1.444177
C	-2.129899	-0.485854	-1.452797
C	-1.438846	0.861745	1.979177
C	-2.107058	1.216278	0.893446
C	-0.722068	2.056116	-1.557222
C	0.605923	2.046284	-1.555411
C	1.449833	-1.628971	-1.529417
C	2.084501	-0.462435	-1.536481
C	2.086391	1.246609	0.820074
C	1.598745	0.968681	2.076095
C	0.028058	-2.406394	0.920780
C	0.034420	-1.637962	1.998038
Ti	1.415035	-0.743469	0.517865
Ti	2.355670	1.391225	-1.047444
Ti	0.019201	-2.783652	-0.972172
Ti	0.050769	0.063061	2.966703
Ti	-1.421818	-0.822747	0.594281
Ti	-0.035486	-0.023922	-1.823857
Ti	0.022218	1.619738	0.500032
Ti	-2.428886	1.370043	-1.003513
C	2.119764	1.286242	3.465655
O	3.128371	1.882768	3.741279
O	1.243958	0.776616	4.334234
Ti_8C_{12}-CO_2 (*B*)			
C	-1.455727	-1.585246	-1.482457
C	-2.125406	-0.438109	-1.496064
C	-1.452440	0.827981	1.995056
C	-2.138519	1.190774	0.917149
C	-0.732373	2.114848	-1.503580
C	0.604907	2.075933	-1.531480
C	1.452876	-1.584158	-1.480767
C	2.106602	-0.440052	-1.483347
C	2.055472	1.236972	0.815923
C	1.639127	0.874694	2.073831
C	0.008490	-2.433789	0.859451
C	-0.045512	-1.683315	1.938669
Ti	1.592110	-0.868119	0.670297
Ti	2.346907	1.425936	-1.028607
Ti	0.003291	-2.768045	-1.031694
Ti	0.025159	-0.048155	2.952130
Ti	-1.421545	-0.816224	0.549641
Ti	-0.013933	0.024829	-1.760449
Ti	0.000183	1.614031	0.513855
Ti	-2.428524	1.408513	-0.981041
C	2.257628	-0.185064	2.852409
O	2.908804	-1.072951	2.123310
O	1.739258	-0.434217	4.007799

Ti_8C_{12}-CO_2 (*C*)			
C	-1.468157	-1.617201	-1.373312
C	-2.145722	-0.480442	-1.312793
C	-1.287745	0.743956	2.151806
C	-2.004883	1.141971	1.115661
C	-0.740203	2.055819	-1.368149
C	0.582884	2.091208	-1.480745
C	1.425670	-1.577881	-1.561633
C	2.082351	-0.424429	-1.614696
C	2.171310	1.207711	0.811528
C	1.594761	0.804154	1.936969
C	0.136584	-2.450785	0.924368
C	0.177598	-1.714407	2.020892
Ti	1.507317	-0.823204	0.477532
Ti	2.352176	1.417040	-1.095710
Ti	0.027958	-2.775944	-0.980224
Ti	0.198440	-0.090569	3.108937
Ti	-1.319418	-0.865811	0.677482
Ti	-0.050796	0.019507	-1.748603
Ti	0.056447	1.610930	0.607157
Ti	-2.431098	1.349630	-0.760564
C	-0.903805	-0.836960	4.773935
O	0.186319	-0.201826	5.059291
O	-1.749301	-1.375947	5.422154
Ti_8C_{12}-CO_2 (*D*)			
C	-1.450705	-1.602078	-1.521926
C	-2.115009	-0.449712	-1.507511
C	-1.491945	0.863401	2.078726
C	-2.125929	1.228727	0.947556
C	-0.668244	2.058085	-1.508448
C	0.661880	2.059841	-1.523294
C	1.466810	-1.605326	-1.415935
C	2.125165	-0.464145	-1.416361
C	2.067569	1.320198	0.888348
C	1.366016	1.017486	1.952720
C	-0.105968	-2.447372	0.889756
C	-0.194749	-1.687917	1.953731
Ti	1.508768	-0.868219	0.773072
Ti	2.397160	1.405864	-1.011254
Ti	-0.015757	-2.776645	-1.009692
Ti	0.028040	-0.013170	2.932349
Ti	-1.442577	-0.771342	0.514176
Ti	0.035368	-0.019145	-1.744972
Ti	-0.052554	1.638099	0.513276
Ti	-2.412293	1.393220	-0.962282
C	2.078897	-1.196391	2.751965
O	2.972436	-1.712143	2.048407
O	1.837803	-1.056872	3.956667

Ti_8C_{12}-CO_2 (*E*)			
C	-1.447079	-1.596464	-1.394371
C	-2.112409	-0.445510	-1.380331
C	-1.410366	0.863755	2.026656
C	-2.126235	1.279841	0.981652
C	-0.720310	2.124407	-1.451676
C	0.612001	2.080276	-1.473874
C	1.473743	-1.671090	-1.497972
C	2.100259	-0.494264	-1.505278
C	2.139683	1.217258	0.862742
C	1.504311	0.836644	1.955267
C	0.065942	-2.512411	0.935395
C	0.073771	-1.703656	1.995340
Ti	1.473776	-0.882377	0.543503
Ti	2.375106	1.376684	-1.050252
Ti	0.010279	-2.825605	-0.974251
Ti	0.069051	-0.005157	2.949196
Ti	-1.283991	-0.758804	0.612519
Ti	0.007985	0.015202	-1.613706
Ti	-0.015323	1.693617	0.574923
Ti	-2.445574	1.422779	-0.922430
C	0.000021	-0.086485	6.339704
O	0.041846	-0.048095	5.177820
O	-0.040068	-0.123664	7.484791

Table S9 Comparison of the relative energies of Ti_8C_{12}-CO_2 complexes obtained using different levels of XC functionals and LDZ basis set.

	Relative energy (eV)				
Isomer	B3LYP	PBE	PBE0	PBE0+GD3	PBE0+BSSE
A	0.00	0.03	0.00	0.00	0.00
B	0.09	0.00	0.00	0.02	0.05
C	0.42	0.74	0.62	0.67	0.46
D	0.74	0.73	0.86	0.86	0.86
E	0.98	1.01	0.77	0.77	0.57

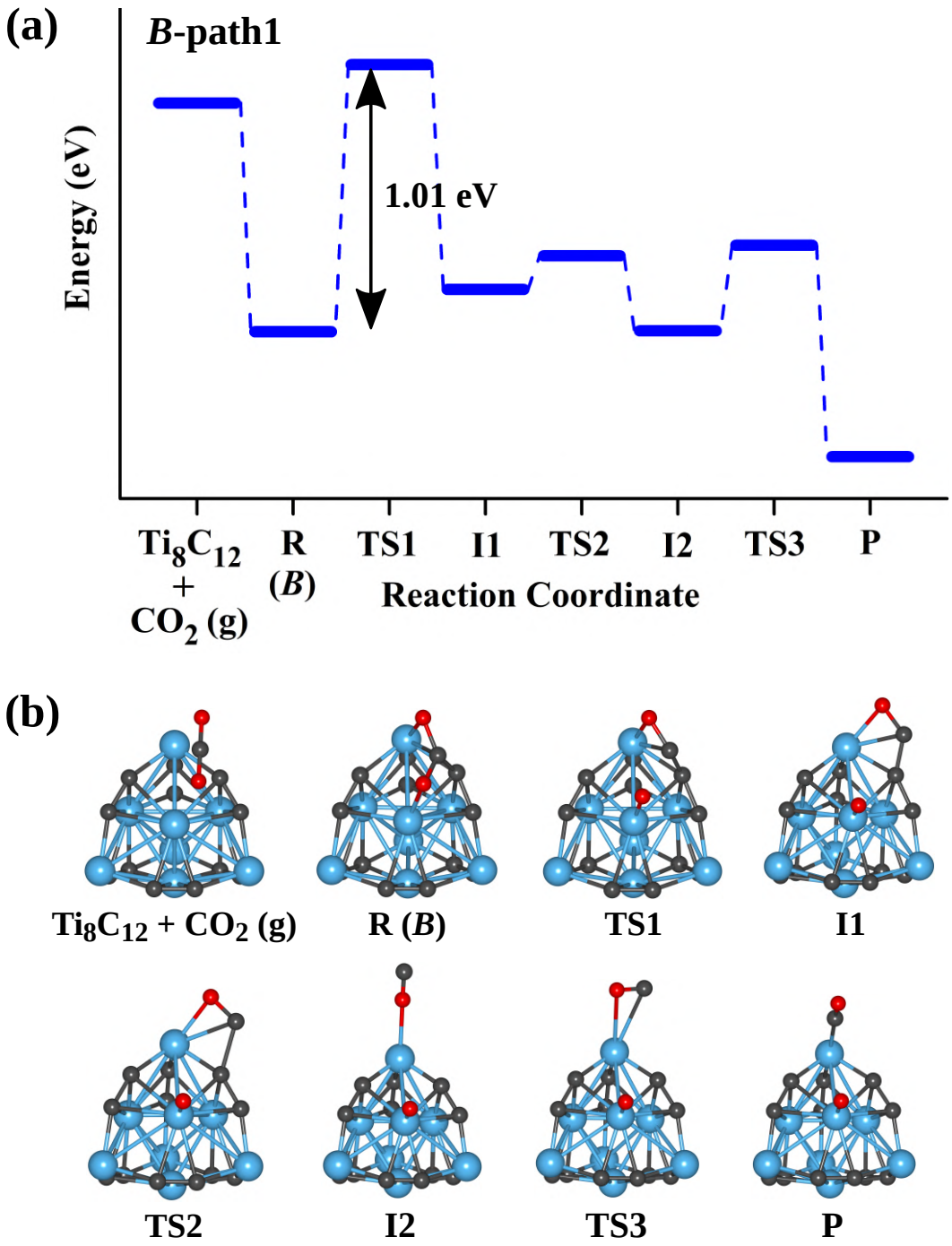

Fig. S7 (a) Reaction path (*B*-path1) for CO_2 dissociation to CO and O fragments on Ti_8C_{12} metcar obtained using B3LYP XC functional and LDZ basis set. TS1, TS2, and TS3 represents the cleavage of C-O bond and the diffusion of CO and O fragments. (b) Optimized structures for dissociation of CO_2 on Ti_8C_{12} metcar. Blue, grey, and red balls represent Ti, C, and O atoms, respectively.

References

[1] N. Blessing, S. Burkart and G. Ganteför, *Eur. Phys. J. D*, 2001, **17**, 37–41.

[2] P. Liu, J. A. Rodriguez, H. Hou and J. T. Muckerman, *J. Chem. Phys.*, 2003, **118**, 7737–7740.

[3] T. Baruah, M. R. Pederson, M. L. Lyn and A. W. Castleman, *Phys. Rev. A*, 2002, **66**, 053201.

[4] L. R. Brock and M. A. Duncan, *J. Phys. Chem.*, 1996, **100**, 5654–5659.

[5] L.-S. Wang, S. Li and H. Wu, *J. Phys. Chem.*, 1996, **100**, 19211–19214.

[6] H. Chen, M. Feyereisen, X. P. Long and G. Fitzgerald, *Phys. Rev. Lett.*, 1993, **71**, 1732–1735.

[7] J. R. Schmidt, N. Shenvi and J. C. Tully, *J. Chem. Phys.*, 2008, **129**, 114110.

[8] E. B. Wilson, J. C. Decius and P. C. Cross, *Molecular vibrations: The theory of infrared and Raman vibration spectra*, New York: McGraw-Hill, 1955.

[9] W. J. Hehre, L. Radom, P. v. R. Schleyer and J. A. Pople, *Ab Initio molecular orbital theory*, Wiley, New York, 1986.

[10] D. van Heijnsbergen, G. von Helden, M. A. Duncan, A. J. A. van Roij and G. Meijer, *Phys. Rev. Lett.*, 1999, **83**, 4983–4986.

[11] J. A. Pople, A. P. Scott, M. W. Wong and L. Radom, *Isr. J. Chem.*, 1993, **33**, 345–350.

[12] A. Alvarez-Garcia, E. Flórez, A. Moreno and C. Jimenez-Orozco, *Mol. Catal.*, 2019, 110733–110741.

[13] A. E. Green, J. Justen, W. Schöllkopf, A. S. Gentleman, A. Fielicke and S. R. Mackenzie, *Angew. Chem. Int. Ed.*, 2018, **57**, 14822–14826.